



ELSEVIER

Contents lists available at ScienceDirect

Developmental Biology

journal homepage: www.elsevier.com/locate/developmentalbiology

A role for tuned levels of nucleosome remodeler subunit ACF1 during *Drosophila* oogenesis

Kenneth Börner^a, Dhawal Jain^a, Paula Vazquez-Pianzola^b, Sandra Vengadasalam^a, Natascha Steffen^a, Dmitry V. Fyodorov^c, Pavel Tomancak^d, Alexander Konev^e, Beat Suter^b, Peter B. Becker^{a,*}

^a Biomedical Center and Center for Integrated Protein Science Munich, Ludwig-Maximilians-University, Munich, Germany

^b Institute of Cell Biology, University of Bern, 3012 Bern, Switzerland

^c Albert Einstein College of Medicine, Cell Biology, Bronx, NY 10461, USA

^d Max Planck Institute of Molecular Cell Biology and Genetics, D-01307 Dresden, Germany

^e Department of Radiation and Molecular Biophysics, St. Petersburg Nuclear Physics Institute, Gatchina 188300, Russia

ARTICLE INFO

Article history:

Received 15 September 2015

Received in revised form

11 December 2015

Accepted 31 January 2016

Keywords:

Nucleosome remodeling

ISWI ATPase

Gerarium

PHD finger

Bromodomain

ABSTRACT

The Chromatin Accessibility Complex (CHRAC) consists of the ATPase ISWI, the large ACF1 subunit and a pair of small histone-like proteins, CHRAC-14/16. CHRAC is a prototypical nucleosome sliding factor that mobilizes nucleosomes to improve the regularity and integrity of the chromatin fiber. This may facilitate the formation of repressive chromatin. Expression of the signature subunit ACF1 is restricted during embryonic development, but remains high in primordial germ cells. Therefore, we explored roles for ACF1 during *Drosophila* oogenesis. ACF1 is expressed in somatic and germline cells, with notable enrichment in germline stem cells and oocytes. The asymmetrical localization of ACF1 to these cells depends on the transport of the *Acf1* mRNA by the Bicaudal-D/Egalitarian complex. Loss of ACF1 function in the novel *Acf1*⁷ allele leads to defective egg chambers and their elimination through apoptosis. In addition, we find a variety of unusual 16-cell cyst packaging phenotypes in the previously known *Acf1*¹ allele, with a striking prevalence of egg chambers with two functional oocytes at opposite poles. Surprisingly, we found that the *Acf1*¹ deletion – despite disruption of the *Acf1* reading frame – expresses low levels of a PHD-bromodomain module from the C-terminus of ACF1 that becomes enriched in oocytes. Expression of this module from the *Acf1* genomic locus leads to packaging defects in the absence of functional ACF1, suggesting competitive interactions with unknown target molecules. Remarkably, a two-fold overexpression of CHRAC (ACF1 and CHRAC-16) leads to increased apoptosis and packaging defects. Evidently, finely tuned CHRAC levels are required for proper oogenesis.

© 2016 Elsevier Inc. All rights reserved.

1. Introduction

The ATPase Imitation Switch (ISWI) is the catalytic core of nucleosome remodeling factors that induce nucleosome sliding on DNA and thus enable structural adjustments of chromatin required to utilize the genome and to maintain its integrity (Baldi and Becker, 2013; Clapier and Cairns, 2009; Mueller-Planitz et al., 2013). Among the six ISWI complexes currently known in *Drosophila melanogaster*, NURF, NoRC and ToRC are prominently involved in transcription activation (Alkhatib and Landry, 2011;

Emelyanov et al., 2012; Vanolst et al., 2005). RSF, ACF and CHRAC on the other hand, are thought to use their nucleosome remodeling activity to close gaps in nucleosomal arrays during chromatin assembly or after disruption, and thus improve the stability and the folding of the chromatin fiber (Fyodorov et al., 2004; Hanai et al., 2008; Ito et al., 1997; Racki et al., 2009; Varga-Weisz et al., 1997). Yeast CHRAC, the Isw2 complex, slides nucleosomes to restrict nucleosome-free regions and represses cryptic transcription that would otherwise originate within these gaps (Whitehouse et al., 2007; Yadon et al., 2010). ACF and CHRAC are highly related complexes. Both are composed of ISWI and the larger signature subunit ACF1, but CHRAC contains two small histone-fold subunits CHRAC-14 and CHRAC-16 in addition (Corona et al., 2000; Ito et al., 1999). *In vitro*, both factors catalyze similar nucleosome sliding reactions (Hartlepp et al., 2005).

* Correspondence to: Ludwig-Maximilians-University, Biomedical Center, Molecular Biology Division, Großhaderner Strasse 9, 82152 Munich, Germany, Tel.: +49 89 2180 75 428; fax: +49 89 2180 75 425.

E-mail address: pbecker@med.uni-muenchen.de (P.B. Becker).

Physiological roles for CHRAC and ACF are poorly understood. To some extent the combined functions of these two related complexes have been assessed by characterization of a loss-of-function mutation of the *Acf1* gene in the *Acf1¹* and *Acf1²* alleles (Chioda et al., 2010; Fyodorov et al., 2004). These studies showed that loss of ACF1 in *Drosophila* embryos reduces the regularity of nucleosome arrays and leads to defects in chromatin-mediated repression processes, such as heterochromatin formation and polycomb silencing. ACF1-deficient embryos also show replication defects indicated by shortened S phases (Fyodorov et al., 2004). Altogether, loss of ACF1 results in 'semi-lethality' during larva-pupae transition and delayed development (Fyodorov et al., 2004).

Acf1 mutant animals show chromatin defects at all developmental stages. Remarkably however, ACF1 is expressed prominently only in undifferentiated cells, which led to the speculation that high levels of ACF1 are a hallmark of unstructured, plastic chromatin in undifferentiated cells prior to developmental epigenome diversification (Chioda et al., 2010). During embryogenesis ACF1 expression fades in most cells and only remains high in neuroblasts and primordial germ cells (PGCs) (Chioda et al., 2010). PGCs are the precursors of the adult germline. However, it is unknown whether high levels of ACF1 are also retained in adult germline tissues. We now have studied the fate of ACF1 in *Drosophila* oogenesis and describe developmentally associated phenotypes in germline and somatic cells by altering ACF1 levels.

Drosophila oogenesis is particularly suited to study germline stem cell (GSC) and somatic stem cell (SSC) renewal, oocyte determination and specification as well as egg formation and maturation. The formation and maturation of eggs occurs in tubular ovarioles. Their most anterior end bears a structure called germarium with 2–3 GSCs in their niche. GSCs divide asymmetrically to produce another stem cell and a daughter cystoblast. Next, cystoblasts undergo four mitotic divisions with incomplete cytokinesis to form an interconnected 16-cell cyst. Importantly, one particular cell is determined to become the oocyte while the remaining 15 cells transform into polyploid nurse cells as cysts travel to the posterior end of the germarium. Thereafter, somatic follicle cells encapsulate and package 16-cell cysts, which bud off as individual egg chambers. Further, egg chamber maturation runs through different developmental stages in which aberrations can be easily scored due to the stereotype positions and appearance of the oocyte and the 15 nurse cells in each egg chamber (Hudson and Cooley, 2014).

Given the widespread requirement for chromatin plasticity during development (Chioda and Becker, 2010; Ho and Crabtree, 2010), it is not surprising that nucleosome remodeling factors have been found important for oogenesis. The nucleosome remodeling ATPases ISWI, Brahma and Domino have been shown to be required for self-renewal of GSCs and SSCs, respectively (Ables and Drummond-Barbosa, 2010; Deuring et al., 2000; He et al., 2014; Xi and Xie, 2005; Yan et al., 2014), conceivably due to their effects on transcription programs.

We now found that ACF1 is expressed in most somatic and germline cells of the female reproductive system with particular high levels in GSCs and oocytes. *Acf1* mRNA enrichment in prospective oocytes is accomplished by the Bicaudal-D/Egalitarian RNA transport machinery. ACF1 is required for proper oogenesis since its loss in a novel, true loss-of-function mutant, *Acf1⁷*, or through RNA interference leads to increased numbers of defective egg chambers. Notably, the well-studied *Acf1¹* allele gives rise to compound egg chamber phenotypes. This allele had hitherto been thought to represent a clear loss-of-function mutation. We now found that this allele still expresses a PHD-Bromo domain module from the ACF1 C-terminus that interferes with 16-cell cyst encapsulation. Remarkably, altering ACF/CHRAC levels by additional gene copies of *Acf1* and *Chrac-16* also interferes with egg chamber

maturation. Evidently, finely tuned CHRAC levels are required for proper oogenesis.

2. Materials and methods

2.1. *Drosophila* strains and genetics

Oregon-R and *w1118* were used as wild type controls. *Acf1* alleles *Acf1¹* and *Acf1²* were described earlier (Fyodorov et al., 2004). In this study the *Acf1⁷* allele was generated by imprecise excision of the *P{EP}Acf1^{EP1181}* P-element previously used to isolate the *Acf1¹* allele. A total of 198 excision events were analyzed by PCR across the *Acf1* locus. Resulting deletions were analyzed by PCR with *Acf1-F* and *Acf1-R* primers that flank the insertion site followed by sequencing with *Acf1-seq* primer (Table S1). The *Acf1⁷* allele carries a 3098 bp deletion (3R:31,794,683–31,797,780) that spans the first intron starting from the *P{EP}Acf1^{EP1181}* insertion site and a part of the third exon of the *Acf1* gene. A 34 bp sequence (CATGATGAAATATCTGAAATATCAATGAAATGTC) of unknown origin was inserted into this region. *Acf1* deficiency (#26539, *w[1118]; Df(3R)BSC687/TM6C, Sb[1] cu[1]*) and *Chrac-16^{G659}* (#33532, *w[*] P{w[+mC]=EP}Chrac-16[G659]*) were obtained from Bloomington *Drosophila* Stock Center (BDSC), USA.

The *Acf1* fosmid variants are based on the fosmid library clone *pflyfos021945* and the *Chrac-16* fosmid on *pflyfos016131*. The genomic region of *Acf1* and *Chrac-16* were modified by recombineering in *Escherichia coli* using the pRedFLP4 recombination technology (Ejsmont et al., 2009). All oligonucleotides and oligonucleotide combinations are listed in Supplementary material (Tables S1 and S2). *Acf1-GFP* fosmid (*Acf1-fos*) codes for full-length ACF1 (1-1476 aa) with a C-terminal 2xTY1-EGFP-3xFLAG-tag. *Acf1-N-GFP* fosmid (*Acf1-N-fos*) codes for ACF1 lacking the C-terminal PHD1, PHD2 and bromodomain (1-1055 aa) with a C-terminal 2xTY1-EGFP-3xFLAG-tag. *Acf1-C-GFP* fosmid (*Acf1-C-fos*) codes only for the C-terminal part of ACF1 (1022-1476 aa) with an N-terminal 2xTY1-EGFP-3xFLAG-tag. *Chrac-16-mCherry* fosmid (*Chrac-16-fos*) codes for full-length CHRAC-16 (1-140 aa) with an N-terminal 2xTY1-mCherry-3xFLAG-tag. A detailed description of the protocol can be obtained from the authors. All *Acf1* and *Chrac-16* fosmid variants were verified by sequencing before injection into *D. melanogaster*. Transgenic flies were made by phiC31 integrase-mediated site-specific integration into attP landing sites (Genetic Services, Inc., USA). *Acf1* fosmid constructs were integrated on the second chromosome into attP40 landing site and *Chrac-16* fosmid construct on the third chromosome into attP2 landing site. Fosmid constructs contain a *dsRed* cassette driven by 3xP3 promoter to select for transformants.

The following homozygous fly lines containing fosmid constructs were obtained by appropriate crosses: *Acf1-fos*, *Acf1-N-fos*, *Acf1-C-fos*, *Acf1-fos*; *Acf1¹*, *Acf1-N-fos*; *Acf1¹*, *Acf1-C-fos*; *Acf1¹*, *Acf1-fos*; *Acf1⁷*, *Acf1-N-fos*; *Acf1⁷*, *Acf1-C-fos*; *Acf1⁷*, *Chrac-16-fos*, *Acf1-fos*; *Chrac-16-fos*, *Acf1-N-fos*; *Chrac-16-fos*, *Acf1-C-fos*; *Chrac-16-fos*.

Short hairpin RNA constructs for *UAS-shAcf1* (JF01298, attP2, Val1; GL00124, attP40, Val22), *UAS-shIswi* (HMS00628, attP40, Val20) and *UAS-shChrac-16* (HMC02362, attP2, Val20) were obtained from the TRiP at Harvard Medical School, Boston, USA. *UAS-shEGFP* (#41557, attP40 Val22), *MTD-Gal4* (#31777) and *mata4-Gal4* (#7063) were obtained from BDSC, USA. *c587-Gal4* and *traffic jam-Gal4* were kind gifts of Allan C. Spradling (Carnegie Institution for Science, USA) and Jean-René Huynh (Institut Curie, France), respectively. *UAS-shRNA* males were crossed with *Gal4* driver virgins at 29°C and 5–7 day old F1 females were used for analysis. For a germline-specific reduction of ISWI in adult ovaries *UAS-shIswi* males were crossed with *MTD-Gal4* driver females at 18°C. F1 females were kept at 29°C for 3 days and used for further analysis.

Generation of *Bic-D^{mom}* flies was done as previously described (Swan and Suter, 1996; Vazquez-Pianzola et al., 2014). Briefly, *Df(2L)Exel7068/SM6B;hs-Bic-D* flies were crossed to *Bic-D⁵/SM1* flies. The progeny of this cross was heat shocked twice per day for 2 h at 37 °C until they reached adulthood. Adults were heat shocked at least for one day before stopping the treatment to shut off *Bic-D* expression.

All fly stocks were kept at 25 °C and ovaries of 5–7 day old females were used for analysis. Individual egg chambers of stage 3–10 were scored for morphological defects from three biological replicates. Mean values in % with SD were calculated for apoptotic and packaging phenotypes.

2.2. Egg laying assay

Female virgins for *Acf1¹*, *Acf1⁷*, *Acf1-fos*; *Acf1¹*, *Acf1-fos*; *Acf1⁷* and *w1118* were collected for 2–3 days at 25 °C. Six females of each genotype were mated with six *w1118* males in vials with yeast paste for 2 days. Females were put in individual vials for 24 h without males and laid eggs were counted. The egg laying capacity was determined as the number of laid eggs per female and day. The data of six females was averaged and mean values with SD from three biological replicates were calculated.

2.3. In situ hybridization to whole mount ovaries

Linearized EST LD32807 (Berkley Drosophila Genome Project, BDGP, USA) containing the *Acf1* cDNA and pBS-Bic-D-short were used as templates to generate digoxigenin-labeled and FITC labeled RNA antisense probes, respectively. *In situ* hybridizations were performed as described (Vazquez-Pianzola et al., 2014).

2.4. Immunological techniques and microscopy

Immunofluorescence microscopy was performed using standard procedures with the following primary antibodies: rat α -ACF1 8E3 [1:2, (Chioda et al., 2010)], mouse α -Orb 6H4 and 4H8 [1:60, Developmental Studies Hybridoma Bank (DHSB), USA], mouse α -Fasciclin III 7G10 (1:100, DHSB), mouse α -HtsRC (1:20, DHSB), mouse α -UNC93-5.2.1 (γ H2A.V, 1:1000, DHSB), rabbit α -Vasa (1:100, Santa Cruz Biotechnology), rabbit α -cleaved Caspase-3 (1:100, Cell Signaling Technology, USA) and rabbit α -GFP TP401 (1:500, Acris Antibodies, Germany). F-actin was visualized with Rhodamine-conjugated phalloidin (1:500, Invitrogen). DAPI (0.1 mg/ml, 1:500) or Hoechst (2 μ g/ml) was used to stain DNA. The following secondary antibodies from Jackson Immuno Research laboratories were used: Donkey α -mouse Cy3 (1:250), Donkey α -mouse Alexa488 (1:300), Donkey α -rat Alexa488 (1:300) and Donkey α -rabbit Alexa488 (1:300). GFP and mCherry fluorescence in flies expressing recombiner fosmid constructs were detected without secondary antibodies in unfixed ovaries, which were stained with DAPI for 10 minutes and washed twice with PBS for 2 min. Imaging was performed with a Leica TCS SP5 II confocal microscope. Images were processed using ImageJ (NIH, USA) and Adobe Photoshop.

2.5. Western blot

For ovary samples, 12 pairs of ovaries were dissected and homogenized in 1 \times Laemmli buffer with a pestle and incubated at 95 °C for 5 min. For embryo samples, nuclear extracts were made from 0–12 hour old embryos (Kunert and Brehm, 2008). Western blot was performed using standard procedures with the following antibodies: rat α -ACF1 8E3 [1:20, (Chioda et al., 2010)], rabbit α -ISWI (1:1000, kind gift from J. Tamkun), mouse α -Lamin T40 (1:2000, kind gift from H. Saumweber). For LI-COR Odyssey

system detection, goat α -rat IgG 800CW, goat α -mouse IgG 680RD and goat α -rabbit IgG 800CW (1:10000, LI-COR Biosciences) were used as secondary antibodies.

2.6. RNA quantification from ovary tissues via real-time PCR

Ovary tissues of wild type, *Acf1¹* and *Acf1⁷* flies were collected in PBS at 4 °C, quickly transferred to Trizol reagent (Qiazol, Qiagen) and frozen at –80 °C. The tissues were then homogenized using electric pestle in a low-binding Eppendorf tube. Next steps were done following the manufacturer's recommendations. Total RNA was extracted using RNeasy Mini kit (Qiagen). On-column DNase digestion was performed using RNase free DNase (Qiagen) to digest genomic DNA. RNA was quantified with a Nanodrop device (Thermo Scientific) and aliquots were frozen at –80 °C. cDNA was prepared using SuperScript[®] III First-Strand Synthesis System (Life technologies). RNase-H (NEB) was used to digest RNA-DNA hybrids. cDNA was subsequently quantified with Fast SYBR-Green (Applied Biosystems) on LightCycler 480 system (Roche). All oligonucleotides are listed in Supplementary material (Table S3).

3. Results

3.1. ACF1 is enriched in cells of the female germline

Monoclonal antibody 8E3 reacts specifically with ACF1 as demonstrated by lack of immunofluorescence staining of *Acf1* mutant embryos and absence of the ACF1 Western blot signal upon probing mutant embryo extracts (Chioda et al., 2010). Using this antibody we previously showed that ACF1 expression is strongly reduced during embryogenesis but persists in primordial germ cells (Chioda et al., 2010). Probing ovarioles from wild type flies we found by immunofluorescence microscopy (IFM) that ACF1 was expressed in most somatic and germline cells of the germarium and the maturing egg chambers (Fig. 1A). Comparison of the fluorescence intensity showed that ACF1 was considerably enriched in the GSCs and possibly the first cystoblast descendant (Fig. 1B, C) with a notable absence in the somatic filament cells, cap cells and anterior escort cells that contribute to forming the stem cell niche (Fig. 1B, C). In contrast to somatic niche cells, ACF1 was expressed in somatic posterior escort cells and all stages of follicle cell development (Fig. 1B, D and E). Further, prominent enrichment of ACF1 staining was seen in the oocyte in stage one 16-cell cysts, soon after the oocyte becomes determined (Fig. 1D). The enrichment of ACF1 in the oocyte nucleus versus the nuclei of polytenic nurse cells continued to be striking in all later egg chambers (Fig. 1A, E). ACF1 was present, but not particularly enriched on the karyosome, and strongly accumulated in the oocyte nucleoplasm (Fig. S1E). The 8E3 antibody provides a novel tool for staining the GSCs and oocytes in the female germline of *Drosophila*.

A common mechanism for asymmetric localization of proteins in prospective oocytes is the transport and localization of their respective mRNAs through an RNA-binding machinery organized by Bicardal-D (*Bic-D*) and Egalitarian (*Egl*) (Claußen and Suter, 2005; Vazquez-Pianzola and Suter, 2012). Indeed, we found by fluorescence *in situ* hybridization (FISH) that *Acf1* mRNA, like its protein product, localized to the prospective oocyte from early stages on (Fig. 1F). The mRNA was present in the nurse and follicle cell cytoplasm and enriched at the posterior cortex of the oocyte cytoplasm from stage 1 of oogenesis onwards and then relocalized to the anterior cortex by stage 8 (Fig. S1A–D), like many of the *Bic-D/Egl* targets. A similar localization pattern was previously observed for *Iswi* mRNA (Jambor et al., 2015). To test whether *Acf1* mRNA transport to the oocyte depends on the *Bic-D/Egl*

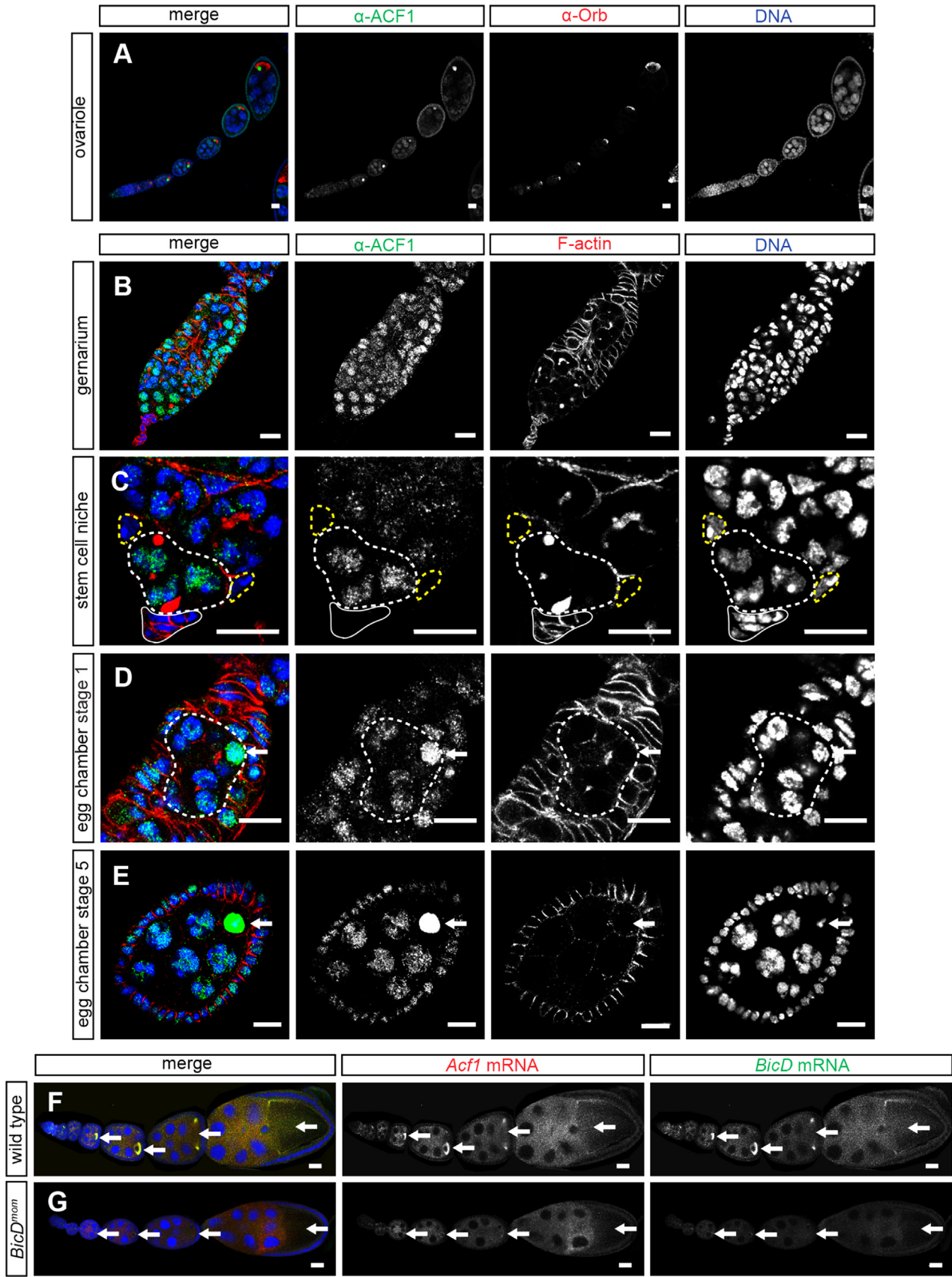


Fig. 1. ACF1 enrichment in germline cells of *Drosophila* ovarioles. (A–E) Immunofluorescence images of different oogenesis stages in wild type. (A) Ovariole with staining of ACF1 (green), Orb (red) and DNA (blue) is shown. (B) Germarium, (C) stem cell niche with cap cells (solid line), germline stem cells (GSCs, white dashed line) and anterior escort cells (yellow dashed line), (D) egg chamber stage 1 (dashed line) and (E) egg chamber stage 5 with staining of ACF1 (green), F-actin (red) and DNA (blue) are shown. Arrows indicate oocyte nuclei. Scale bar: 10 μ m. (F–G) *In situ* hybridization with staining of *Acf1* mRNA (red), *BicD* mRNA (green) and DNA (blue) is shown for the following genotypes: (F) wild type and (G) *Bic-D^{mom}*. Arrows indicate oocyte nuclei. Scale bar: 20 μ m.

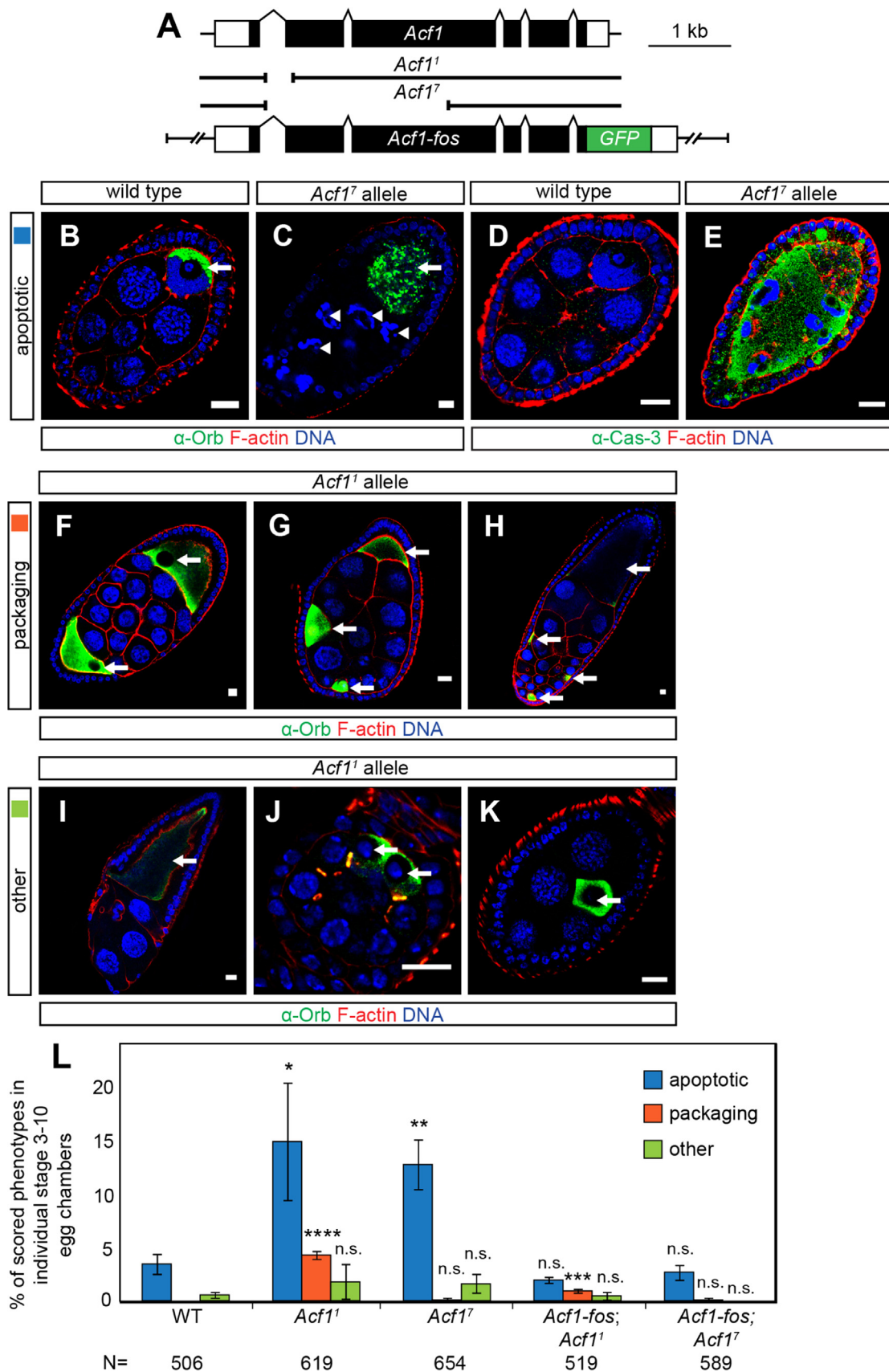


Fig. 2. *Acf1* alleles give rise to oogenesis phenotypes. (A) Schematic representation of the *Acf1* gene, *Acf1*¹ and *Acf1*⁷ genomic deletions and the *Acf1* fosmid construct. White and black rectangles represent untranslated and translated exons, respectively. Green rectangle shows inserted 2xTY1-GFP-3xFLAG-tag. (B-E) Immunofluorescence images of apoptotic phenotype. Representative egg chambers of the *Acf1*¹ allele with staining of (B, C) Orb (green), F-actin (red) and DNA (blue) and (D, E) cleaved Caspase-3 (green), F-actin (red) and DNA (blue) are shown for wild type and the *Acf1*⁷ allele. Arrows indicate oocyte nuclei. Arrowheads indicate nurse cell nuclei. Scale bar: 10 μ m. (F-H) Immunofluorescence images of packaging phenotypes. Representative egg chambers of the *Acf1*¹ allele with staining of Orb (green), F-actin (red) and DNA (blue) are shown for the *Acf1*¹ allele. Egg chambers with additional cysts and two (F), three (G) and four oocytes (H) are shown. (I-K) Immunofluorescence images of other phenotypes. Egg chambers with one oocyte and seven nurse cells (I), two adjacent oocytes (J) and delocalized oocyte (K) are shown. Arrows indicate oocyte nuclei. Scale bar: 10 μ m. (K) Quantification of apoptotic, packaging and other phenotypes. The data show mean values in percent with SD of three biological replicates. N represents the total number of scored egg chambers stage 3-10. Two-tailed Student's *t*-test was used in comparison to wild type. * represents a *p*-value of < 0.05, ** < 0.01, *** < 0.001 and **** < 0.0001. n.s. represents not significant.

localization machinery, we depleted the germline of Bic-D protein after oocyte determination using *Bic-D^{mom}* flies (Swan and Suter, 1996; Vazquez-Pianzola et al., 2014). The *Bic-D^{mom}* tool involves rescuing the *Bic-D^{null}* phenotype by adding a copy of *Bic-D* under an inducible heat shock promoter. Once the oocyte determination phenotype had been rescued, induction of *Bic-D* expression was stopped. Around 4 days later these ovaries contained mid-oogenesis egg chambers lacking *Bic-D* mRNA (Fig. 1G) and protein (Vazquez-Pianzola et al., 2014). We found the oocyte enrichment of the *Acf1* mRNA severely impaired in these egg chambers (Fig. 1G) indicating that *Acf1* is a novel target of the RNA transport machinery.

3.2. Egg chamber formation and maturation phenotypes associated with *Acf1* alleles

To explore potential roles for ACF in oogenesis, we analyzed ovarioles from two *Acf1* homozygous mutant fly lines. The *Acf1¹* allele had been considered a null allele (Fyodorov et al., 2004). It is characterized by a short deletion of parts of the first intron and second exon (Fig. 2A), which disrupts the reading frame. We also characterized a novel allele, *Acf1⁷*, which bears a larger deletion of 3098 bp in the *Acf1* coding sequence (Fig. 2A; see Section 2) generated by imprecise excision of *P{EP}Acf1^{EP1181}* P-element.

We analyzed ovarioles of wild type, *Acf1¹* and *Acf1⁷* flies by staining the cytoplasmic oocyte marker Orb, along with DNA and F-actin. Orb marks the single oocyte at the posterior end of wild type 16-cell cysts. We scored individual egg chambers stage 3–10 and found two distinct categories of morphological abnormalities. The largest fraction (*Acf1¹*: 16%; *Acf1⁷*: 13%; apoptotic defects, Fig. 2L) consisted of egg chambers in the process of decay in which oocyte and nurse cells appeared in various stages of apoptosis (Fig. 2B and C) as verified by staining for activated caspase-3 (Fig. 2D and E). Interestingly, the increased number of apoptotic cysts only appeared from stage 7 or 8 onwards (Fig. S2A–D) while oogenesis appeared normal in the germarium (Fig. S2E–G). In theory, ACF1 loss could affect chromosome maturation and morphology, which might be identified as defects in oocyte nuclei condensation and nurse cell polyteny. However, such chromatin derangements were not scored (Fig. S2H–K). Staining with the DNA double strand break marker γ H2A.V might reveal even subtle chromatin defects if they predispose *Acf1* chromosomes to DNA damage. However, we did not detect any major difference in γ H2A.V staining patterns or intensities between wild type and *Acf1⁷* ovarioles (Fig. S2L–U).

More interestingly, a significant number of about 5% of all egg chambers in *Acf1¹* showed various deficiencies in 16-cell cyst packaging (packaging defects; Fig. 2L). The most striking packaging phenotype, which was often observed, revealed two oocytes at the opposite poles of the egg chamber (Fig. 2F), which is reminiscent of compound egg chamber phenotypes reported in other studies (Besse et al., 2002; Hawkins et al., 1996; Jackson and Blochlinger, 1997; McGregor et al., 2002; Urwyler et al., 2012). Both oocytes appeared equivalent as they were positive for Orb (Fig. 2F), showed correctly positioned nuclei in close proximity to epithelial follicle and nurse cells (Fig. 2F) and contained four ring canals (Fig. S3A–D). Other variations of compound egg chamber phenotypes were also observable, such as three or four oocytes at opposing positions with nurse cells of different size and ploidy (Fig. 2G, H). Similar packaging phenotypes were also seen analyzing the *Acf1²* deletion allele (data not shown), which had been generated independently from the *Acf1¹* allele by imprecise excision of a different P-element (Fyodorov et al., 2004). Compound egg chambers were observed at all stages of maturation, including the earliest egg chamber stage 1 (Fig. S3F). In principle, such an arrangement may come about if two adjacent germline cysts are

packaged together into one egg chamber by somatic follicle cells. Indeed, in many cases more than one cyst was encapsulated by follicle cells in *Acf1¹* (Fig. S3E, F). Furthermore, only *Acf1¹* but not *Acf1⁷* germaria showed additional FasIII-positive stalk-like structures and egg chambers with additional, wrongly positioned polar cells (Fig. S3G–L). Surprisingly however, compound eggs were never scored in *Acf1⁷* (Fig. 2L). We hypothesize that the two *Acf1* alleles are not equivalent: some aspects of *Acf1¹* appear to lead to packaging phenotypes that are not characteristic of *Acf1⁷*.

In a third category, about 2% of all egg chambers in *Acf1¹* and *Acf1⁷* showed a wide variety of abnormalities such as egg chambers with one oocyte and seven nurse cells (Fig. 2I), two adjacent oocytes (Fig. 2J) and centralized oocytes (Fig. 2K). However, the penetrance of these other abnormalities in *Acf1¹* and *Acf1⁷* was not significantly different from wild type and therefore excluded from further analysis (Fig. 2L).

We next focused on the analysis of apoptotic and packaging phenotypes in ovariole structures to better understand the effect of *Acf1* alleles on *Drosophila* oogenesis and fertility. We found defective ovarioles significantly increased in both *Acf1* alleles in comparison to wild type (wild type: 12%, *Acf1¹*: 32%, *Acf1⁷*: 20%; Fig. S4A). It is thought that apoptotic egg chambers at the posterior end of an ovariole can interrupt egg production in individual ovarioles or throughout the entire ovary (Thomson et al., 2010), which should lead to a decreased number of laid eggs in both *Acf1* alleles. In fact, apoptotic egg chambers were found almost exclusively to be the most posterior egg chamber (*Acf1¹*: 20/21, *Acf1⁷*: 38/38; Fig. S2B, C) and females of both *Acf1* alleles showed a significant reduction in egg laying to less than 85% in comparison to wild type (Fig. S4C). In summary, both *Acf1* alleles show defective egg chambers and compromise female fertility.

To verify that the observed oogenesis phenotypes are due to mutations in the *Acf1* gene locus we crossed the *Acf1¹* and *Acf1⁷* alleles to an *Acf1* deficiency. Indeed, this confirmed the penetrance of apoptotic and packaging phenotypes in both *Acf1* alleles (Fig. S4B). We further validated the observed phenotypes by generating a transgene expressing GFP-tagged *Acf1* from a recombined fosmid (*Acf1-fos*) using the flyfosmid recombineering technique (Ejmont et al., 2009). This way, we obtained a fly line expressing GFP-tagged ACF1 from its chromosomal regulatory context (Fig. 2A). *Acf1-fos* was integrated into the attP40 landing site on the 2nd chromosome by PhiC31-mediated recombination and used to complement the *Acf1* alleles. We found GFP-tagged ACF1 expressed in ovarioles by Western blot (Fig. S5A). In comparison to the two specific ACF1 signals detected in wild type, we found the expected higher molecular weight band only in ACF1-GFP complemented flies. The lower ACF1-specific band, which was present in wild type and ACF1-GFP complemented flies, most likely represents C-terminally truncated ACF1. We also confirmed that ACF1-GFP localized to GSCs, oocytes, follicle and nurse cells by IFM using a GFP antibody (Fig. S5B–G). Importantly, expression of an ACF1-GFP transgene fully rescued all apoptotic defects in *Acf1¹* and *Acf1⁷* allele and packaging defects were ameliorated in *Acf1¹* (Fig. 2L).

3.3. ACF1 depletion in early phases of oogenesis manifests itself in later egg chamber phenotypes

To better understand the consequences of loss of ACF function for oogenesis, we depleted ACF1 and its partner ISWI by cell type-specific RNA interference (RNAi) using the Gal4/UAS system (Ni et al., 2011). ACF expression was interfered with by expressing small hairpin (sh) RNAs directed against *Acf1* or *Iswi* mRNA under the control of UAS system. Expression was driven in the germline cells by using *MTD* or *mata4* (Yan et al., 2014) and in the somatic cells by *c587* (Eliazer et al., 2011; Kai and Spradling, 2003) or *traffic*

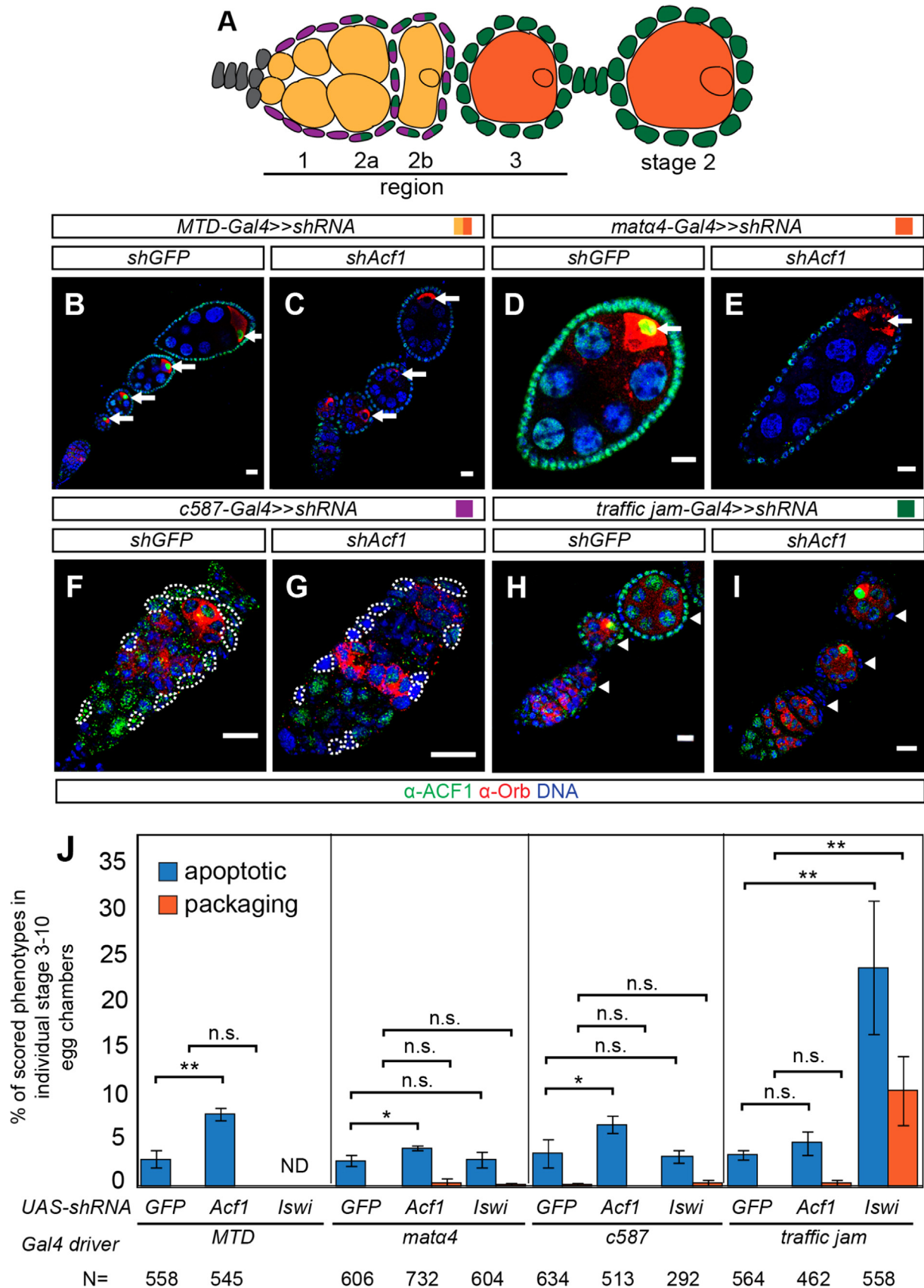


Fig. 3. Cell type-specific RNAi-mediated knockdown of ACF subunits in oogenesis causes apoptotic and packaging phenotypes. (A) Schematic drawing of early *Drosophila* oogenesis. Color code for cell type-specific expression pattern of different driver lines: *MTD-Gal4* (germline cells; light and dark orange), *mata4-Gal4* (germline cells stage 1 onwards, dark orange), *c587-Gal4* (somatic escort and early follicle cells, purple) and *traffic jam-Gal4* (somatic follicle cells, green). (B–I) Immunofluorescence images showing cell type-specific ACF1 knockdown in oogenesis. Germarium, ovariole or egg chamber with staining of ACF1 (green), Orb (red) and DNA (blue) are shown for: (B) *UAS-shGFP* < < *MTD-Gal4* (C), *UAS-shAcf1* < < *MTD-Gal4* (D) *UAS-shGFP* < < *mata4-Gal4*, (E) *UAS-shAcf1* < < *mata4-Gal4*, (F) *UAS-shGFP* < < *c587-Gal4*, (G) *UAS-shAcf1* < < *c587-Gal4*, (H) *UAS-shGFP* < < *traffic jam-Gal4* and (I) *UAS-shGFP* < < *traffic jam-Gal4*. Arrows indicate oocyte nuclei. White dashed lines indicate escort cells. Color-coded square represents specific cell-type expression pattern in Fig. 3A. Scale bar: 10 μ m. (J) Quantification of apoptotic and packaging phenotypes. The data show mean values in percent with SD of three biological replicates. *N* represents the total number of scored egg chambers stage 3–10. All analyzed ovary samples of *shIswi* with *MTD-Gal4* (*n* = 14) showed an agametic phenotype but detailed oogenesis phenotypes were not determined (ND) further. Two-tailed Student's *t*-test was used. * represents a *p*-value of < 0.05 and ** < 0.01. n.s. represents not significant.

jam Gal4 drivers (Olivieri et al., 2010) (Fig. 3A). As a control for non-specific effects we expressed shRNA directed against an irrelevant GFP sequence with the same drivers. This did not affect ACF1 levels (Fig. 3B, D, F and H) and led to a low rate of apoptotic egg chambers (Fig. 3J) similar to wild type flies (Fig. 2L).

MTD-directed knockdown of ACF1 expression in germline cells (Fig. 3C; Fig. S6A and B) increased the number of apoptotic egg chambers from stage 7 or 8 onwards to about 8% (Fig. 3J; Fig. S6E, F). However, *mat α 4*-mediated knockdown showed a small, statistically significant increase in apoptotic phenotype of unclear physiological relevance (4%, Fig. 3J). Under this circumstance ACF1 was virtually absent from germline cells but still detectable on follicle cells from stage 2 egg chambers onwards (Fig. 3E; Fig. S6C, D). Similarly, removal of ACF1 from follicle cells but not from germline cells with *traffic jam-Gal4* (Fig. 3I; Fig. S7C, D) did not have an effect (Fig. 3J). In contrast, ACF1 depletion in somatic escort and early follicle cells with *c587-Gal4* (Fig. 3G; Fig. S7A, B) caused a modest, two-fold increase in apoptotic egg chambers from stage 7 or 8 onwards (7%; Fig. 3J; Fig. S7E, F). The penetrance of apoptotic phenotypes scored upon early germline and soma knockdown of ACF1 could sum up to the observed apoptotic phenotypes in the *Acf1¹* and *Acf1⁷* allele (Fig. 2L). Remarkably, we did not observe any packaging defects of the kind scored with the *Acf1¹* allele (Fig. 3J).

Interfering with the expression of the ATPase ISWI through similar crosses might more generally reveal the cell type-specific importance of ISWI complexes for oogenesis. As expected, ablation of ISWI in early germline cells with *MTD-Gal4* yielded an agametic phenotype with characteristically small ovaries and defects in early oogenesis (data not shown; Fig. 3J) (Ables and Drummond-Barbosa, 2010; Xi and Xie, 2005; Yan et al., 2014). Interestingly, knockdown with *mat α 4-Gal4* did not cause any pronounced phenotype (Fig. 3J), arguing for a requirement for ISWI complexes primarily in early phases of cyst formation. To circumvent the requirement for ISWI function in early germline development we repeated the cross of *MTD-Gal4* with *shIswi* at 18 °C and put F1 offspring females to 29 °C for three days. We reasoned that a reduction of ISWI in adult germline cells should increase the penetrance of apoptotic egg chambers at least to levels comparable to a germline-specific *Acf1* knockdown. Indeed, an ISWI reduction in adult germline cells revealed an increased number of apoptotic egg chambers (64%, Fig. S8A) and induced packaging defects (14%, Fig. S8B). This further indicates that a loss of ACF1 function compromises oogenesis as part of the ISWI-containing ACF complex. However, the penetrance of apoptotic egg chambers was considerably higher suggesting a contribution of other ISWI-containing remodeling complexes.

Next, we focused on the phenotypical analysis of ISWI reduction in all stages of follicle cell development using the *traffic jam-Gal4* driver, which led to strongly increased numbers of apoptotic egg chambers (25%; Fig. 3J), induced a considerable number of packaging defects (11%; Fig. 3J), and yielded a 'dumpless' phenotype with short eggs (58%; Fig. S8K). Surprisingly, some of these packaging defects were reminiscent of *Acf1¹* allele phenotypes, including compound egg chambers (Fig. S8C). However, even more complex packaging phenotypes with three and more oocytes in non-opposing positions were frequently scored (Fig. S8D). In contrast to *Acf1¹* phenotypes, ISWI ablation in follicle cells gave rise to many egg chambers with abnormal cell numbers ranging from only one to eight cells (Fig. S8E, F and I). These egg chambers had fewer ring canal connections (Fig. S8F) and were already observed in region 2a/b of the germarium (Fig. S8G, I). This could argue for a soma-dependent early germline defect in cell proliferation. Furthermore, we also found gaps in the follicle cell epithelium (Fig. S8I) and additional stalk-like structures (Fig. S8J) that could lead to packaging defects (Fig. S8H). In contrast,

reduction of ISWI in somatic escort and early follicle cells in the germarium via *c587-Gal4* showed no phenotype (Fig. 3J). So far, ISWI function has not been considered critical in follicle cell development (Xi and Xie, 2005).

3.4. Germline-specific enrichment of an ACF1 remnant from the *Acf1¹* allele

The RNA interference phenotype resembled the phenotype of the *Acf1⁷* allele. We therefore considered that *Acf1¹* may not be a true 'null' allele. Since the *Acf1* promoter and first exon are intact in the *Acf1* alleles (Fig. 2A) it is likely that mRNA is transcribed. Indeed, we found some *Acf1* gene sequences transcribed in ovaries from the *Acf1¹* and *Acf1⁷* alleles, however with lower levels in comparison to wild type (Fig. S9A). We speculated that a small C-terminal fragment of ACF1 may be translated from an internal methionine in the *Acf1¹* but not in the *Acf1⁷* allele. This was addressed using the monoclonal 8E3 antibody that recognizes an epitope in the ACF1 C-terminus (aa 1064-1476; data not shown). As expected, this antibody did not detect the two specific ACF1 bands by Western blot analysis of ovary extract from either of the two mutants (Fig. 4A). Despite all efforts, a low molecular weight band specific for the ACF1 C-Terminus was not detectable in *Acf1¹* and *Acf1⁷* ovary extracts (data not shown). Remarkably, however, the ACF1 antibody yielded a robust immunofluorescence signal in oocyte nuclei of *Acf1¹* mutant egg chambers, including the two oocytes of compound egg chambers (Fig. 4B, C). In contrast, ACF1 C-terminal immunoreactivity was absent in *Acf1⁷* egg chambers (Fig. 4B, D). Any stable 3' parts of *Acf1* mRNA transcribed from the *Acf1¹* allele are expected to be processed by the RNA transport machinery, since the 3' UTR remains intact. Indeed, we found *Acf1*-derived mRNA localized and enriched in the oocyte only in *Acf1¹* and *Acf1²* mutant egg chambers, including both oocytes of compound egg chambers (Fig. 4E, data not shown), but not in the *Acf1⁷* allele (Fig. 4G). We conclude that *Acf1¹* is not a 'null' allele, but rather expresses a portion of the ACF1 C-terminus that enriches in germline cells. It is, therefore, possible that packaging phenotypes are due to the presence of an out-of-context ACF1 fragment.

3.5. Ectopic expression of the ACF1 C-terminus leads to compound egg chamber phenotypes

The comparison of the effects of *Acf1¹* and *Acf1⁷* alleles on oogenesis and the detection of *Acf1* mRNA and protein only in *Acf1¹* led to the hypothesis that the former allele produces a C-terminal ACF1 fragment. The ACF1 C-terminus bears two prominent PHD fingers and a bromodomain, for which no target is known. Conceivably, expressing this module may interfere with critical functions by competing with other, yet unknown factors for shared interaction sites. In order to test this hypothesis more directly, we used transgenic fly lines containing fosmids which express GFP-tagged *Acf1-N* and *Acf1-C* termini (*Acf1-N-fos*, *Acf1-C-fos*, Fig. 5A). The N-terminal ACF1 fragment (ACF1-N) contains the domains required to interact with ISWI (Eberharter et al., 2004) and the CHRAC-14/16 heterodimer (Hartlepp et al., 2005), but lacks the PHD-bromo module (Fig. 5B). Conversely, the C-terminal ACF1 fragment (ACF1-C) lacks the ISWI interaction surface, but contains the PHD-bromo module (Fig. 5B). *Acf1-N-fos* and *Acf1-C-fos* were made by flyfosmid recombineering technique and integrated on the 2nd chromosome at the same site as the fosmid expressing full-length ACF1-GFP. Interestingly, ACF1-N was not specifically enriched in the oocyte (Fig. 5D). However, ACF1-C was not only expressed in follicle and nurse cells but also enriched in oocyte nuclei (Fig. 5E), in agreement with the earlier results of RNA FISH in *Acf1¹* mutant ovarioles (Fig. 4F).

Acf1-N-fos and *Acf1-C-fos* were tested in the background of wild

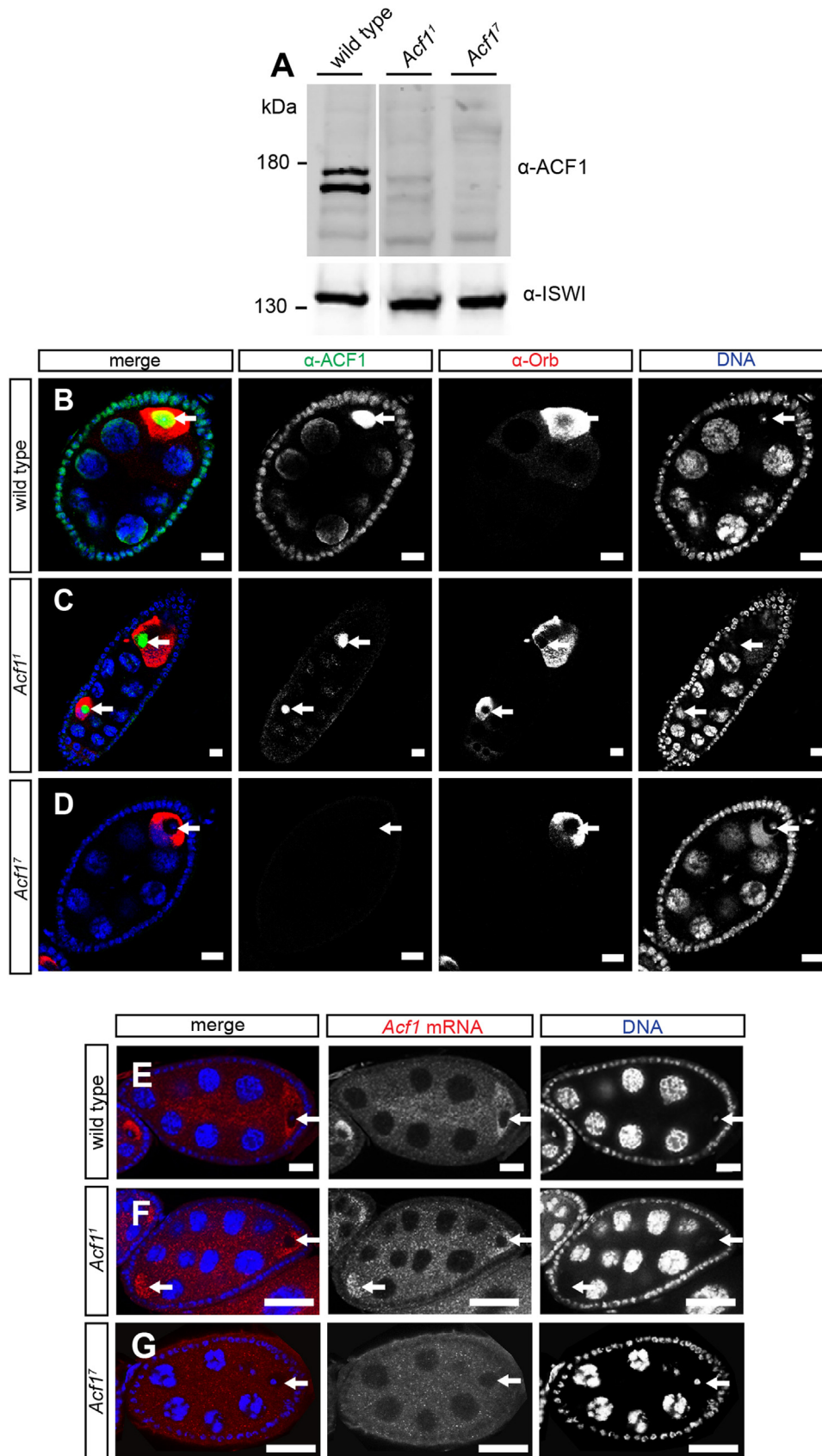


Fig. 4. Germline-specific enrichment of the ACF1 C-terminus from the *Acf1¹* allele. (A) Western blot from ovaries probed with α -ACF1 8E3 is shown for the following homozygous genotypes: wild type, *Acf1¹* and *Acf1⁷*. ISWI signal served as a loading control. (B–D) Immunofluorescence images of egg chambers with staining of ACF1 (green), Orb (red) and DNA (blue) are shown for the following homozygous genotypes: (B) wild type, (C) *Acf1¹* and (D) *Acf1⁷*. Arrows indicate oocyte nuclei. Scale bar: 10 μ m. (E–G) *In situ* hybridization with staining of *Acf1* mRNA (red) and DNA (blue) is shown for the following homozygous genotypes: (E) wild type, (F) *Acf1¹* and (G) *Acf1⁷*. Arrow indicates oocyte. Scale bar: 20 μ m.

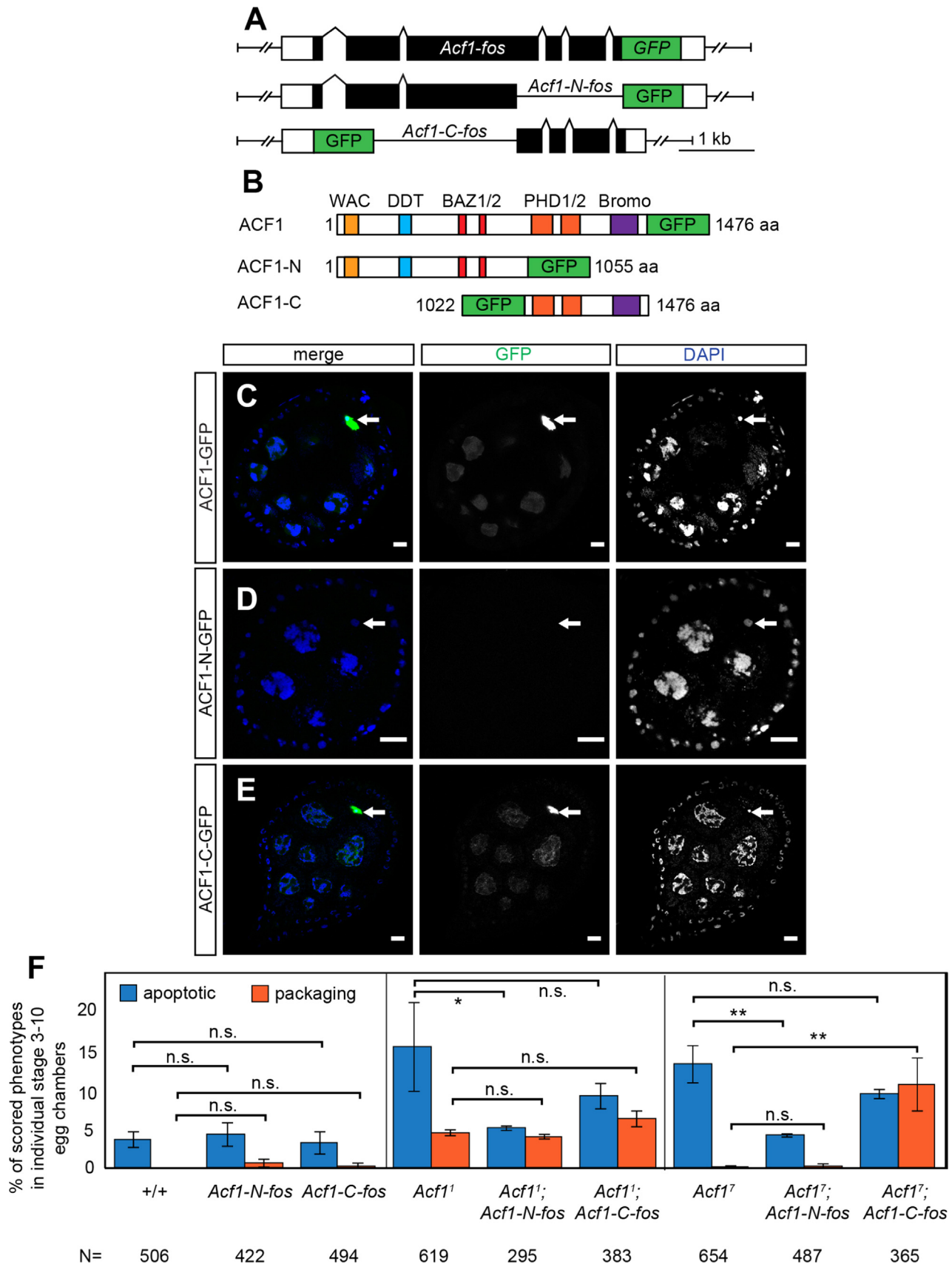


Fig. 5. Ectopic expression of the ACF1 C-terminus leads to compound egg chamber phenotypes. (A) Schematic representation of the *Acf1-C* and *Acf1-N* fosmid constructs. White and black rectangles represent untranslated and translated exons, respectively. Green rectangles show inserted 2xTY1-GFP-3xFLAG-tag. (B) Schematic representation of domain structure of ACF1-C and ACF1-N. Green rectangles show inserted 2xTY1-GFP-3xFLAG-tag. (C-E) Live cell fluorescence images of egg chambers from fly lines expressing tagged *ACF1-GFP* constructs showing GFP (green) and DNA (blue) signal. (A) *ACF1-GFP*, (B) *ACF1-N-GFP* and (C) *ACF1-C-GFP* are shown. Arrows indicate oocyte nuclei. Scale bar: 10 μ m. (F) Quantification of apoptotic and packaging phenotypes. The data show mean values in percent with SD of three biological replicates. *N* represents the total number of scored egg chambers stage 3–10. Two-tailed Student's *t*-test was used. * represents a *p*-Value of < 0.05 and ** < 0.01. n.s. represents not significant.

type, *Acf1*¹ and *Acf1*⁷ alleles for oogenesis phenotypes and particularly for the occurrence of packaging defects. Neither ACF1-N nor ACF1-C had a dominant negative effect, since neither of them showed increased apoptotic phenotypes in wild type background (Fig. 5F). Curiously, the presence of ACF1-N reduced the occurrence of apoptotic egg chambers in both *Acf1* alleles to wild type levels (*Acf1*¹: 2%; *Acf1*⁷: 1%; Fig. 5F). However, ACF1-N did not ameliorate packaging phenotypes in *Acf1*¹ (4%, Fig. 5F). The ACF1 N-terminus, containing the CHRAC-16 and ISWI interaction domains, was sufficient to rescue the apoptotic phenotype, conceivably as part of ACF/CHRAC complexes. We repeated cell-type specific RNAi for CHRAC-16 and used an insertion mutant allele, *P{EP}Chrac-16^{G659}*, to test for the contribution of CHRAC-16 to ACF/

CHRAC phenotypes. In brief, we did not observe apoptotic phenotypes with CHRAC-16 RNAi or *Chrac-16^{G659}* (Fig. S10A, B) supporting a more prominent role of ACF1 during oogenesis than for CHRAC-16.

The ACF1 C-terminus did not rescue apoptotic phenotypes as expected (Fig. 5F). Strikingly, however, the presence of ACF1-C in *Acf1*⁷ induced packaging defects, including compound egg chambers (10%; Fig. 5F). In conclusion, ACF1-N, containing CHRAC and ISWI interaction domains, is sufficient to rescue the apoptotic phenotype in *Acf1* alleles, while ACF1-C, containing a PHD-bromo module, induces packaging defects only in the absence of full-length ACF1.

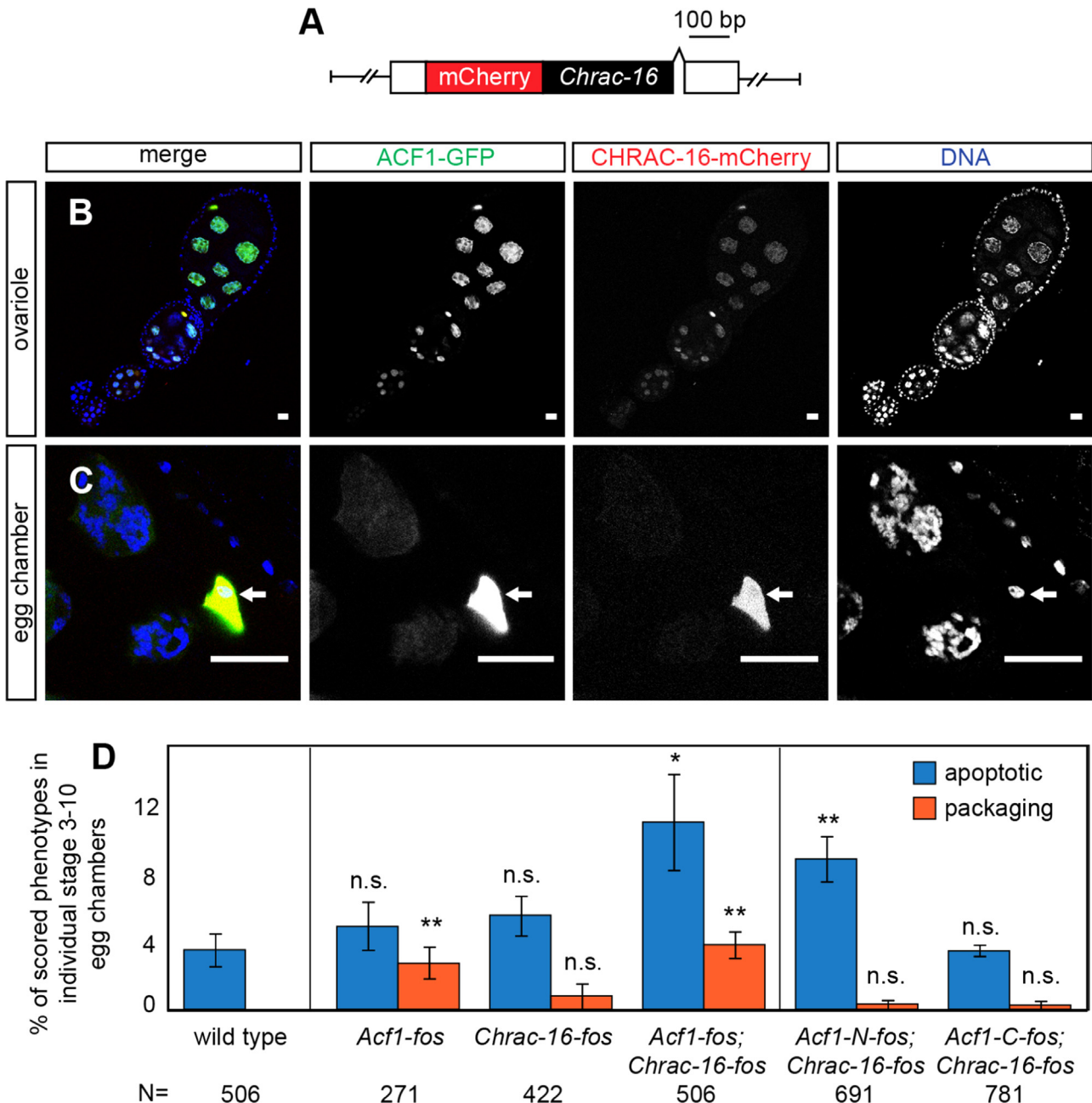


Fig. 6. Tuned ACF1 and CHRAC levels are critical for oogenesis. (A) Schematic representation of the *Chrac-16* fosmid construct. White and black rectangles represent untranslated and translated exons, respectively. Red rectangle shows inserted 2xTY1-mCherry-3xFLAG-tag. (B, C) Live cell fluorescence images of fly line expressing tagged ACF1-GFP and CHRAC-16-mCherry with GFP (green), mCherry (red) and DNA signal (blue) are shown. Arrows indicate oocyte nuclei. Scale bar: 10 μ m. (D) Quantification of apoptotic and packaging phenotypes. The data show mean values in percent with SD of three biological replicates. N represents the total number of scored egg chambers stage 3-10. Two-tailed Student's *t*-test was used in comparison to wild type. * represents a *p*-Value of < 0.05 and ** < 0.01. n.s. represents not significant.

3.6. Tuned ACF1 and CHRAC-16 levels are critical for oogenesis

The results from the expression of ACF1 fragments suggest that packaging phenotypes may arise from competitive interactions of isolated domains with yet undefined targets. Conceivably, such untargeted interactions may interfere with other remodeling processes. We wondered whether such competition might also happen if full-length ACF1 or the small CHRAC-16 signature subunit of CHRAC was overexpressed. However, it is only poorly understood whether ACF1 functions in ACF or CHRAC *in vivo*. Despite all efforts, we were unable to raise a specific CHRAC-16 antibody suitable for IFM. Therefore, we generated a fly line bearing a fosmid expressing mCherry-tagged CHRAC-16 from its native genomic context (*Chrac-16-fos*, Fig. 6A) to study the localization of CHRAC complex in oogenesis. We detected both ACF1-GFP and CHRAC-16-mCherry signals in nurse cells and oocytes of all stages (Fig. 6B and C). This finding suggests that the four-subunit CHRAC complex localizes to the female germline.

To test for competitive interactions of excess full-length ACF1, we analyzed the ovarioles of flies bearing two copies of the ectopic, tagged *Acf1* gene locus in addition to endogenous *Acf1* genes. Indeed, these flies expressed approximately a double dose of ACF1 analyzed by quantitative Western blotting (2.6 fold; Fig. S5E). Remarkably, increased ACF1 levels led to a low, yet statistically significant number of packaging defects (3%; Fig. 6D), including compound egg chambers.

Moreover, homozygous *Acf1-fos*; *Chrac-16-fos* flies carrying four copies of *Acf1* and *Chrac-16* genes showed an increased number of apoptotic egg chambers (12%; Fig. 6D) with packaging defects similar to *Acf1-fos* (4%; Fig. 6D). However, no further increase in apoptosis was observed with additional copies of either *Acf1* or *Chrac-16-fosmid* (Fig. 6D). This finding suggests that excess CHRAC interferes with proper oogenesis. This hypothesis was further addressed by combination of *Chrac-16-fosmid* with *Acf1-N* or *Acf1-C-fosmid*. Indeed, increased apoptotic defects were only observed in combination of ACF1-N-*fos* with *Chrac-16-fos* (9%; Fig. 6D) but not with ACF1-C-*fos* which lacks the CHRAC-16 interaction domain (3%; Fig. 6D). We conclude that combining elevated levels of ACF1 and CHRAC-16 poses a risk for oogenesis failure.

Our data suggest that the *Acf1*⁷ allele represents a true loss-of-function phenotype, best described as a variegated failure to assemble viable egg chambers. Failed attempts are removed through apoptosis. Expression of the N-terminal portion of ACF1 rescues this phenotype. By contrast, the interesting packaging defects found in *Acf1*¹ alleles are presumably due to interference of an out-of-context ACF1 interaction module. In support of this conclusion, we found that expression of ACF1-C in an *Acf1*⁷ background induces packaging phenotypes, including compound egg chambers. Remarkably, a mild overexpression of CHRAC leads to increased apoptotic and packaging defects. Indicating that, finely tuned CHRAC levels are required for proper oogenesis.

4. Discussion

The highly related nucleosome remodeling complexes ACF and CHRAC are prototypic nucleosome sliding factors. Their biochemical activities are very similar and their physiological functions thought to be highly related. The available information suggests that these factors do not contribute to regulating gene expression, but fulfill more general tasks in the assembly and maintenance of properly packaged chromatin fibers with regular nucleosome spacing. Their high and global expression during early embryogenesis may be rationalized by a presumed need for such activity during times of extremely rapid replication cycles. Human ACF1 (and by inference the remodelers hACF and hCHRAC) facilitates

replication through heterochromatin (Collins et al., 2002), but recently roles in the signaling and repair of DNA breaks have been described as well (Lan et al., 2010; Sánchez-Molina et al., 2011). An analogous function for the *Drosophila* factors, which may also be beneficial during early embryonic development, has not been reported yet.

With these considerations in mind we were surprised by the rather specific enrichment of ACF1 in the *Drosophila* germline. We had suggested earlier that high levels of ACF1 may indicate a state of chromatin plasticity that is characteristic of undifferentiated cells (Chioda et al., 2010). However, our new finding that ACF1 is expressed in differentiated follicle and nurse cells do not support this hypothesis. The specific enrichment of ACF1 in GSCs and prospective oocytes by the Bicaudal-D/Egalitarian RNA transport machinery suggests specific functions of the remodeler during oogenesis. However, specific ACF1 enrichment in the oocyte nucleoplasm could also hint to requirements of ACF1 in early processes of embryo development (Chioda et al., 2010; Fyodorov et al., 2004).

We analyzed two independent *Acf1* mutant alleles to explore the consequences of ACF1 loss on oogenesis. Both mutants showed an increased level of apoptotic egg chambers from stage 7 or 8 onwards. Similar abortions of egg chambers were also scored if ACF1 had been ablated in either germline or somatic cells, provided that the knockdown was induced early. The abortion of eggs might be promoted by external cues, such as unfavorable environmental conditions or intrinsic factors, such as 'low quality' oocytes (Jenkins et al., 2013; McCall, 2004; Thomson et al., 2010). Following the latter idea, loss of ACF1 remodeling activity might lead to the accumulation of multiple subtle changes in chromatin structure and function that collectively may compromise the execution of gene expression or cell cycle programs critical to the complex oogenesis process.

While we cannot exclude a role for ACF/CHRAC in transcription control, we do not favor such a scenario. Preliminary transcriptome profiling of *Acf1*⁷ mutant embryos does not suggest systematic and direct effects of ACF1 on transcription. Furthermore, ACF1 cannot be trapped by formaldehyde crosslinking at regulatory regions (Jain et al., 2015).

The ACF1 loss-of-function phenotype was neither explained by replication defects that may lead to asynchrony of 16-cell cyst formation or reduced nurse cell ploidy nor by defects in the resolution of meiotic recombination. Such perturbations of the integrity of the chromatin fiber would be detectable by enhanced γ H2A.V staining, which was not observed. The modesty of the failure rate might be explained by functional redundancy, for example with RSF, an ISWI-containing remodeling complex predicted to have very similar functions to ACF/CHRAC (Baldi and Becker, 2013; Loyola et al., 2001; Lusser et al., 2005; Torigoe et al., 2011).

Our findings that depletion of ISWI in early germline cells causes an agametic phenotype and that ISWI functions outside of the germarium are not required for further oocyte differentiation is in agreement with previous observations (Xi and Xie, 2005; Yan et al., 2014). A requirement for the ISWI-containing remodeler NURF for GSC fate and activity had already been described, but this can be explained by the known role of NURF as (co-) regulator of transcription programs (Ables and Drummond-Barbosa, 2010; Xi and Xie, 2005). Besides, ISWI depletion in follicle cells causes a variety of severe packaging defects arguing for a role of ISWI remodeling activity in somatic cells, which had not been considered so far (Xi and Xie, 2005).

Remarkably, we also found a range of interesting 16-cell cyst packaging defects in the related, but independent, *Acf1*¹ and *Acf1*² alleles. These alleles had been assumed loss-of-function alleles, because the small deletions disrupt the reading frame and no

protein is detectable by Western blotting or IFM in mutant embryos. The packaging defects manifested themselves as a variety of compound egg chambers containing more than one 16-cell cyst and often with oocytes prominently placed at opposite poles. This rare phenotype had been described only in a few mutants of different signaling pathways (Besse et al., 2002; Hawkins et al., 1996; Jackson and Blochlinger, 1997; McGregor et al., 2002; Urwyler et al., 2012) and Polycomb genes (Narbonne et al., 2004). The fact that we observe surplus stalk-like structures and polar cells suggests that the morphogenetic abnormalities are due to encapsulation defects.

The depletion of ACF1 by RNAi as well as the true loss-of-function mutation in the *Acf1*⁷ allele never yielded packaging defects. This argues against *Acf1*¹ being a null allele, reiterating earlier concerns (Ables and Drummond-Barbosa, 2010). Our finding of a cell-specific expression of a C-terminal ACF1 fragment containing a prominent PHD-bromo module now provides a molecular explanation for the phenomenon. Indeed, the ectopic expression of this module induced packaging phenotypes in the absence of functional ACF1, suggesting competitive interactions with yet unknown target molecules. Our novel finding that depletion of ISWI in somatic cells also leads to a variety of packaging phenotypes, including compound egg chambers similar to the ones scored in the *Acf1*¹ allele may indicate an interference of the out-of-context ACF1 C-terminus with the function of another ISWI remodeling complex.

Tagging the signature subunit of CHRAC, CHRAC-16, for the first time allowed monitoring its expression *in vivo*. The colocalisation of CHRAC-16 and ACF1 in prospective oocytes and nurse cells suggests a function for CHRAC (as opposed to just ACF) during oogenesis. This notion receives support from the finding that mild combined overexpression of ACF1 and CHRAC-16 generated apoptotic and packaging phenotypes. This leads to the surprising conclusion that proper oogenesis requires that CHRAC levels are finely adjusted within a two-fold range. Whether excess CHRAC interferes with functions of other chromatin regulators by competition with shared targets remains an interesting question and challenge for future research.

Author contributions

KB, DJ, PVP, SV, NS, AK performed experiments; DVF, PT, AK, BS, PBB developed concepts and approaches; KB, PVP, BS, PBB analyzed data; KB, PBB prepared the manuscript; all authors edited the manuscript prior to submission.

Acknowledgments

Stocks obtained from the Bloomington *Drosophila* Stock Center (NIH P40D018537) were used in this study. We thank the TRiP at Harvard Medical School (NIH/NIGMS R01-GM084947) for providing transgenic RNAi fly lines. The monoclonal antibodies Orb 4H8 and 6H4 were developed by Paul Schedl, 7G10 anti-Fasciilin III was developed by Corey Goodman, HtsRC was developed by Lynn Cooley and UNC93-5.2.1 was developed by R. Scott Hawley. They were obtained from the Developmental Studies Hybridoma Bank, created by the NICHD of the NIH and maintained at The University of Iowa, Department of Biology, Iowa City, IA 52242.

We thank Drs. S. Mietzsch, G. Reuter, N.R. Matias and J.R. Huynh for stimulating discussions and advice. We thank B. Schaller, D. Beuchle and Y. Ilina for technical help. M. Chioda participated in the early phase of the project. This work was supported by the Deutsche Forschungsgemeinschaft through Grants Be1140/7-1 and

SFB1064/A01 (PBB), by the Swiss National Science Foundation through Grant 31003A 153280 (BS) and by the Russian Ministry of Science and Education through Grants RF 8131 06.08.2012 and RFBR 15-04-99583 (AK).

Appendix A. Supplementary material

Supplementary data associated with this article can be found in the online version at <http://dx.doi.org/10.1016/j.ydbio.2016.01.039>.

References

- Ables, E.T., Drummond-Barbosa, D., 2010. The steroid hormone ecdysone functions with intrinsic chromatin remodeling factors to control female germline stem cells in *Drosophila*. *Cell Stem Cell* 7, 581–592. <http://dx.doi.org/10.1016/j.stem.2010.10.001>.
- Alkhatib, S.G., Landry, J.W., 2011. The nucleosome remodeling factor. *FEBS Lett.* 585, 3197–3207. <http://dx.doi.org/10.1016/j.febslet.2011.09.003>.
- Baldi, S., Becker, P.B., 2013. The variant histone H2A.V of *Drosophila*—three roles, two guises. *Chromosoma* 122, 245–258. <http://dx.doi.org/10.1007/s00412-013-0409-x>.
- Besse, F., Busson, D., Pret, A.-M., 2002. Fused-dependent Hedgehog signal transduction is required for somatic cell differentiation during *Drosophila* egg chamber formation. *Development* 129, 4111–4124.
- Chioda, M., Becker, P.B., 2010. Soft skills turned into hard facts: nucleosome remodelling at developmental switches. *Heredity* 105, 71–79. <http://dx.doi.org/10.1038/hdy.2010.34>.
- Chioda, M., Vengadasalam, S., Kremmer, E., Eberharter, A., Becker, P.B., 2010. Developmental role for ACF1-containing nucleosome remodellers in chromatin organisation. *Development* 137, 3513–3522. <http://dx.doi.org/10.1242/dev.048405>.
- Clapier, C.R., Cairns, B.R., 2009. The biology of chromatin remodeling complexes. *Annu. Rev. Biochem.* 78, 273–304. <http://dx.doi.org/10.1146/annurev.biochem.77.062706.153223>.
- Claußen, M., Suter, B., 2005. BicD-dependent localization processes: from *Drosophila* development to human cell biology. *Ann. Anat.* 187, 539–553. <http://dx.doi.org/10.1016/j.aanat.2005.07.004>.
- Collins, N., Poot, R. a, Kukimoto, I., García-Jiménez, C., Dellaire, G., Varga-Weisz, P.D., 2002. An ACF1-ISWI chromatin-remodeling complex is required for DNA replication through heterochromatin. *Nat. Genet.* 32, 627–632. <http://dx.doi.org/10.1038/ng1046>.
- Corona, D.F., Eberharter, a, Budde, a, Deuring, R., Ferrari, S., Varga-Weisz, P., Wilm, M., Tamkun, J., Becker, P.B., 2000. Two histone fold proteins, CHRAC-14 and CHRAC-16, are developmentally regulated subunits of chromatin accessibility complex (CHRAC). *EMBO J.* 19, 3049–3059. <http://dx.doi.org/10.1093/emboj/19.12.3049>.
- Deuring, R., Fanti, L., Armstrong, J.A., Sarte, M., Papoulas, O., Prestel, M., Daubresse, G., Verardo, M., Moseley, S.L., Berloco, M., Tsukiyama, T., Wu, C., Pimpinelli, S., Tamkun, J.W., Sapienza, L., Moro, P.A., Genetica, I., 2000. The ISWI chromatin-remodeling protein is required for gene expression and the maintenance of higher order chromatin structure *in vivo*. *Mol. Cell* 5, 355–365.
- Eberharter, A., Vetter, I., Ferreira, R., Becker, P.B., 2004. ACF1 improves the effectiveness of nucleosome mobilization by ISWI through PHD-histone contacts. *EMBO J.* 23, 4029–4039. <http://dx.doi.org/10.1038/sj.emboj.7600382>.
- Ejsmont, R.K., Sarov, M., Winkler, S., Lipinski, K. a, Tomancak, P., 2009. A toolkit for high-throughput, cross-species gene engineering in *Drosophila*. *Nat. Methods* 6, 435–437. <http://dx.doi.org/10.1038/nmeth.1334>.
- Eliazer, S., Shalaby, N.A., Buszczak, M., 2011. causes stem cell tumors in the *Drosophila* ovary 2011. doi:10.1073/pnas.1015874108/-DCSupplemental.www.pnas.org/cgi/doi/10.1073/pnas.1015874108.
- Emelyanov, A.V., Vershilova, E., Ignatyeva, M. a, Pokrovsky, D.K., Lu, X., Konev, A.Y., Fyodorov, D.V., 2012. *Genes Dev.* 26, 603–614. <http://dx.doi.org/10.1101/gad.180604.111>.
- Fyodorov, D.V., Blower, M.D., Karpen, G.H., Kadonaga, J.T., 2004. Acf1 confers unique activities to ACF / CHRAC and promotes the formation rather than disruption of chromatin *in vivo*. *Genes Dev.* 18, 170–183. <http://dx.doi.org/10.1101/gad.1139604>.
- Hanai, K., Furuhashi, H., Yamamoto, T., Akasaka, K., Hirose, S., 2008. RSF governs silent chromatin formation via histone H2Av replacement. *PLoS Genet.* 4, e1000011. <http://dx.doi.org/10.1371/journal.pgen.1000011>.
- Hartlepp, K.F., Fernández-Tornero, C., Eberharter, A., Grüne, T., Müller, C.W., Becker, P.B., 2005. The histone fold subunits of *Drosophila* CHRAC facilitate nucleosome sliding through dynamic DNA interactions. *Mol. Cell. Biol.* 25, 9886–9896. <http://dx.doi.org/10.1128/MCB.25.22.9886>.
- Hawkins, N.C., Thorpe, J., Schüpbach, T., 1996. *Encore*, a gene required for the regulation of germ line mitosis and oocyte differentiation during *Drosophila* oogenesis. *Development* 122, 281–290.
- He, J., Xuan, T., Xin, T., An, H., Wang, J., Zhao, G., Li, M., 2014. Evidence for chromatin-remodeling complex PBAP- controlled maintenance of the *drosophila*

- ovarian germline stem cells. *PLoS One*, 9. <http://dx.doi.org/10.1371/journal.pone.0103473>.
- Ho, L., Crabtree, G.R., 2010. Chromatin remodelling during development. *Nature* 463, 474–484. <http://dx.doi.org/10.1038/nature08911>.
- Hudson, A.M., Cooley, L., 2014. Methods for studying oogenesis. *Methods* 68, 207–217. <http://dx.doi.org/10.1016/j.ymeth.2014.01.005>.
- Ito, T., Bulger, M., Pazin, M.J., Kobayashi, R., Kadonaga, J.T., 1997. ACF, an ISWI-containing and ATP-utilizing chromatin assembly and remodeling factor. *Cell* 90, 145–155.
- Ito, T., Levenstein, M.E., Fyodorov, D.V., Kutach, A.K., Kobayashi, R., Kadonaga, J.T., 1999. assembly ACF consists of two subunits , Acf1 and ISWI , that function cooperatively in the ATP-dependent catalysis of chromatin assembly. *Genes Dev.*
- Jackson, S.M., Blochlinger, K., 1997. cut interacts with Notch and protein kinase A to regulate egg chamber formation and to maintain germline cyst integrity during *Drosophila* oogenesis. *Development* 124, 3663–3672.
- Jain, D., Baldi, S., Zabel, a, Straub, T., Becker, P.B., 2015. Active promoters give rise to false positive “Phantom Peaks” in ChIP-seq experiments. *Nucleic Acids Res.*, 1–10. <http://dx.doi.org/10.1093/nar/gkv637>.
- Jambor, H., Surendranath, V., Kalinka, A.T., Mejsstrik, P., Saalfeld, S., Tomancak, P., 2015. Systematic imaging reveals features and changing localization of mRNAs in *Drosophila* development. *Elife* 4, 1–22. <http://dx.doi.org/10.7554/eLife.05003>.
- Jenkins, V.K., Timmons, A.K., McCall, K., 2013. Diversity of cell death pathways: Insight from the fly ovary. *Trends Cell Biol.* 23, 567–574. <http://dx.doi.org/10.1016/j.tcb.2013.07.005>.
- Kai, T., Spradling, A., 2003. An empty *Drosophila* stem cell niche reactivates the proliferation of ectopic cells. *Proc. Natl. Acad. Sci. U.S.A.* 100, 4633–4638. <http://dx.doi.org/10.1073/pnas.0830856100>.
- Lan, L., Ui, A., Nakajima, S., Hatakeyama, K., Hoshi, M., Watanabe, R., Janicki, S.M., Ogiwara, H., Kohno, T., Kanno, S.I., Yasui, A., 2010. The ACF1 complex is required for dna double-strand break repair in human cells. *Mol. Cell* 40, 976–987. <http://dx.doi.org/10.1016/j.molcel.2010.12.003>.
- Loyola, A., LeRoy, G., Wang, Y.H., Reinberg, D., 2001. Reconstitution of recombinant chromatin establishes a requirement for histone-tail modifications during chromatin assembly and transcription. *Genes Dev.* 15, 2837–2851. <http://dx.doi.org/10.1101/gad.937401>.
- Lusser, A., Urwin, D.L., Kadonaga, J.T., 2005. Distinct activities of CHD1 and ACF in ATP-dependent chromatin assembly. *Nat. Struct. Mol. Biol.* 12, 160–166. <http://dx.doi.org/10.1038/nmsb884>.
- McCall, K., 2004. Eggs over easy: cell death in the *Drosophila* ovary. *Dev. Biol.* 274, 3–14. <http://dx.doi.org/10.1016/j.ydbio.2004.07.017>.
- McGregor, J.R., Xi, R., Harrison, D., 2002. *Development* 129, 705–717.
- Mueller-Planitz, F., Klinker, H., Becker, P.B., 2013. Nucleosome sliding mechanisms: new twists in a looped history. *Nat. Struct. Mol. Biol.* 20, 1026–1032. <http://dx.doi.org/10.1038/nmsb.2648>.
- Narbonne, K., Besse, F., Brissard-Zahraoui, J., Pret, A.-M., Busson, D., 2004. poly-homeotic is required for somatic cell proliferation and differentiation during ovarian follicle formation in *Drosophila*. *Development* 131, 1389–1400. <http://dx.doi.org/10.1242/dev.01003>.
- Ni, J.-Q., Zhou, R., Czech, B., Liu, L.-P., Holderbaum, L., Yang-Zhou, D., Shim, H.-S., Tao, R., Handler, D., Karpowicz, P., Binari, R., Booker, M., Brennecke, J., 2011. *Nat. Methods* 8, 405–407. <http://dx.doi.org/10.1038/nmeth.1592>.
- Olivieri, D., Sykora, M.M., Sachidanandam, R., Mechtler, K., Brennecke, J., 2010. An in vivo RNAi assay identifies major genetic and cellular requirements for primary piRNA biogenesis in *Drosophila*. *EMBO J.* 29, 3301–3317. <http://dx.doi.org/10.1038/emboj.2010.212>.
- Racki, L.R., Yang, J.G., Naber, N., Partensky, P.D., Acevedo, A., Purcell, T.J., Cooke, R., Cheng, Y., Narlikar, G.J., 2009. The chromatin remodeler ACF acts as a dimeric motor to space nucleosomes. *Nature* 462, 1016–1021. <http://dx.doi.org/10.1038/nature08621>.
- Sánchez-Molina, S., Mortusewicz, O., Bieber, B., Auer, S., Eckey, M., Leonhardt, H., 2011. *Nucleic Acids Res.* 39, 8445–8456. <http://dx.doi.org/10.1093/nar/gkr435>.
- Swan, A., Suter, B., 1996. Role of Bicaudal-D in patterning the *Drosophila* egg chamber in mid-oogenesis. *Development* 122, 3577–3586.
- Thomson, T.C., Fitzpatrick, K.E., Johnson, J., 2010. Intrinsic and extrinsic mechanisms of oocyte loss. *Mol. Hum. Reprod.* 16, 916–927. <http://dx.doi.org/10.1093/molehr/gaq066>.
- Torigoe, S.E., Urwin, D.L., Ishii, H., Smith, D.E., Kadonaga, J.T., 2011. Identification of a rapidly formed nonnucleosomal histone-DNA intermediate that is converted into chromatin by ACF. *Mol. Cell* 43, 638–648. <http://dx.doi.org/10.1016/j.molcel.2011.07.017>.
- Urwiler, O., Cortinas-Elizondo, F., Suter, B., 2012. *Drosophila* sosie functions with H-Spectrin and actin organizers in cell migration, epithelial morphogenesis and cortical stability. *Biol. Open* 1, 994–1005. <http://dx.doi.org/10.1242/bio.20122154>.
- Vanolst, L., Fromental-Ramain, C., Ramain, P., 2005. Toutatis, a TIP5-related protein, positively regulates Pannier function during *Drosophila* neural development. *Development* 132, 4327–4338. <http://dx.doi.org/10.1242/dev.02014>.
- Varga-Weisz, P.D., Wilm, M., Bonte, E., Dumas, K., Mann, M., Becker, P.B., 1997. Chromatin-remodelling factor CHRAC contains the ATPases ISWI and topoisomerase II. *Nature* 388, 598–602.
- Vazquez-Pianzola, P., Adam, J., Haldemann, D., Hain, D., Urlaub, H., Suter, B., 2014. Clathrin heavy chain plays multiple roles in polarizing the *Drosophila* oocyte downstream of Bic-D. *Development* 141, 1915–1926. <http://dx.doi.org/10.1242/dev.099432>.
- Vazquez-Pianzola, P., Suter, B., 2012. Conservation of the RNA transport machineries and their coupling to translation control across eukaryotes. *Comp. Funct. Genom.*, 2012. <http://dx.doi.org/10.1155/2012/287852>.
- Whitehouse, I., Rando, O.J., Delrow, J., Tsukiyama, T., 2007. Chromatin remodelling at promoters suppresses antisense transcription. *Nature* 450, 1031–1035. <http://dx.doi.org/10.1038/nature06391>.
- Xi, R., Xie, T., 2005. Stem cell self-renewal controlled by chromatin remodeling factors. *Science* 310, 1487–1489. <http://dx.doi.org/10.1126/science.1120140>.
- Yadon, A.N., Van de Mark, D., Basom, R., Delrow, J., Whitehouse, I., Tsukiyama, T., 2010. Chromatin remodeling around nucleosome-free regions leads to repression of noncoding RNA transcription. *Mol. Cell Biol.* 30, 5110–5122. <http://dx.doi.org/10.1128/MCB.00602-10>.
- Yan, D., Neumüller, R. a, Buckner, M., Ayers, K., Li, H., Hu, Y., Yang-Zhou, D., Pan, L., Wang, X., Kelley, C., Vinayagam, A., Binari, R., Randklev, S., Perkins, L. a, Xie, T., Cooley, L., Perrimon, N., 2014. A regulatory network of *Drosophila* germline stem cell self-renewal. *Dev. Cell* 28, 459–473. <http://dx.doi.org/10.1016/j.devcel.2014.01.020>.